Direct real-space observation of nearly stochastic behavior in magnetization reversal process on a nanoscale

M.-Y. Im,[1] D.-H. Kim,[2] K.-D. Lee,[1] S.-H. Lee,[1] P. Fischer,[3] and S.-C. Shin[1*]

[1]Department of Physics and Center for Nanospinics of Spintronic Materials, Korea Advanced Institute of Science and Technology, Daejeon 305-701, Korea;
[2]Department of Physics, Chungbuk National University, Chungbuk, Korea;
[3]Center for X-ray Optics, Lawrence Berkeley National Laboratory, Berkeley CA94720, USA

Abstract

We report a non-deterministic nature in the magnetization reversal of nanograins of CoCrPt alloy film. Magnetization reversal process of CoCrPt alloy film is investigated using high resolution soft X-ray microscopy which provides real space images with a spatial resolution of 15 nm. Domain nucleation sites mostly appear stochastically distributed within repeated hysteretic cycles, where the correlation increases as the strength of the applied magnetic field increases in the descending and ascending branches of the major hysteresis loop. In addition, domain configuration is mostly asymmetric with inversion of an applied magnetic field in the hysteretic cycle. Nanomagnetic simulation considering thermal fluctuations of the magnetic moments of the grains explains the nearly stochastic nature of the domain nucleation behavior observed in CoCrPt alloy film.

With the bit size in high-densitiy magnetic recording media approaching nanometer length scale, one of the fundamental and crucial issues is whether the domain nucleation during magnetization reversal process exhibits a deterministic behavior. Repeatability of local domain nucleation and deterministic switching behavior are basic and essential factors for achieving high performance in high-density magnetic recording [1-3]. Most experimental studies on this issue reported so far have been mainly performed by

indirect probes through macroscopic hysteresis loop and Barkhausen pattern measurements, which provide the ensemble-average magnetization. Thus, they are inadequate to gain insight into the domain-nucleation behavior on a nanometer length scale during the magnetization reversal process [4-6]. Very recently, coherent X-ray speckle metrology, where the speckle pattern observed in reciprocal space acts as a fingerprint of the domain configurations, was adopted to investigate stochastic behavior in the magnetization reversal of a Co/Pt multilayer film [7,8]. However, no direct observation on the stochastic behavior of domain nucleation during magnetization reversal in real space at the nanometer scale has yet been reported. The main reason is due to limitations of the microscopic measurement techniques employed. Thus, experimental confirmation for stochastic behavior of domain nucleation together with its clarification has to date remained a scientific challenge.

In this Letter we report the first direct observation of nearly stochastic behavior of domain nucleation in real space utilizing high resolution, element-specific, magnetic soft X-ray transmission microscopy (MTXM) [9]. Recent achievements in Fresnel zone plate technology, used as X-ray optical element, provide a lateral resolution of 15 nm in MTXM [10,11]. The sample used in our study is a nanogranular CoCrPt alloy film, which has received significant attention as a potential high-density perpendicular magnetic recording media [12].

To observe the magnetic domain configuration during magnetization reversal process, we have utilized the full-field magnetic transmission soft X-ray microscopy beamline 6.1.2 at the Advanced Light Source in Berkeley CA. The experimental setup of this X-ray microscope is described elsewhere [13]. A condensor zone plate (CZP) with a pinhole close to the sample serves as a linear monochromator with a measured spectral resolution of $E/\Delta E = 700$ near the Co L_3 absorption edge (777 eV). The CZP provides a partially coherent hollow cone illumination of the (ferromagnetic) sample, with circularly polarized radiation emitted off-orbit from the bending magnet. After

transmitting the circularly polarized X-ray through the sample, the images are projected by the micro zone plate objective lens to a 2048 × 2048 pixel backside illuminated CCD, which provides a 15 nm spatial resolution image. X-ray magnetic circular dichroism serves as magnetic contrast mechanism. To distinguish structural contrast due to defects, inhomogeneities, etc., from magnetic contrast, the images were normalized to an image taken under an external field sufficient to saturate the film. 50-nm thick $(Co_{83}Cr_{17})_{87}Pt_{13}$ alloy films were prepared on a 40-nm thick Ti buffer layer using dc magnetron cosputtering of CoCr alloy target and Pt target at a base pressure better than 8×10^{-7} Torr and a sputtering Ar pressure of 3 mTorr at ambient temperature. To allow sufficiently high transmission of soft X-rays, a 200-nm thick Si_3N_4 membrane was used as a substrate. The magnetic anisotropy and the macroscopic magnetic properties were characterized using a torque magnetometer and a vibrating sample magnetometer (VSM), respectively.

Magnetic transmission X-ray microscopy (MTXM) images were recorded at the Co L_3 (777 eV) absorption edge with varying applied magnetic field, generated by a solenoid with field strength up to 5 kOe. The measurement time during the X-ray experiment took usually ~1 sec to get a single-shot full-field image. No noticeable change of domain configuration was observed beyond the measurement time, implying that magnetization reversal process was fully relaxed within the measurement time. All measurements were carried out at room temperature. The magnetic domain configuration taken at an external magnetic field of +400 Oe is displayed together with the M-H hysteresis curve obtained by VSM in Figs. 1(a) and (b). As demonstrated in the figure the magnetization reversal of the CoCrPt sample is governed by the magnetic domain nucleation process. Several nucleation sites with sizes around or less than 40 nm can be observed as dark spots showing up at random positions. The nucleation-mediated process of magnetization reversal observed in this system is believed to reveal switching of individual grains isolated by compositional segregation at grain boundaries based on previous TEM studies of this system [14,15].

To investigate repeatability of domain-nucleation sites during the magnetization reversal process, we recorded magnetic domain configurations at identical applied magnetic field points in several tens of successive hysteretic reversal cycles always starting at a fully saturated state. A topological defect in the sample was used to identify the exact same sample area in sequential images. Typical domain configurations taken at applied magnetic fields of +620, +512, +383, +254, +124, and +5 Oe in the descending branch of the major hysteresis loop during two consecutive hysteretic cycles are illustrated in Fig. 2(a). Interestingly enough, one clearly notes that in most cases the nucleation sites appear different in two consecutive cycles, as representatively shown in the inserted circles. For a better visualization of the randomness of nucleation sites, we have overlapped two domain configuration images in a larger sample area of 7.6×7.6 μm^2 obtained from the consecutive measurements. Fig. 2(b) shows a typical overlapped image taken under an applied magnetic field of +400 Oe, where red and green spots represent the first and second measurements, respectively, and the black spots indicate the coincident nucleation sites between the two measurements. This result clearly reveals that the domain nucleation process of CoCrPt alloy film is not deterministic, but mostly stochastic in the successive hysteretic cycles. This kind of stochastic behavior is also witnessed within the opposite branch of the hysteretic cycle. In Fig. 2(c), we demonstrate the domain configurations at magnetic fields of ±620, ±512, ±383, ±254, ±124, and ±5 Oe in the process of the hysteretic cycle, where the positive and negative signs correspond to the left and right branches of a hysteresis loop. It is clearly seen that, in general, the domain configurations appear asymmetrically with an inversion of the applied field. Figure 2(d) shows an overlapped image of domain configurations in the of 7.6×7.6 μm^2 sample area, where the red and green spots correspond to nucleation sites at positive and negative applied fields of 400 Oe, respectively, and the black spots correspond to the coincident nucleation sites. One clearly sees that nucleation sites mostly appear stochastically with an inversion of the applied field. Thus, no inversion symmetry exists with respect to the applied field direction.

The degree of stochastic behavior of the domain configuration is found to be dependent on the applied magnetic field strength as one notices from Figs. 2(a) and 2(c). To quantitatively examine the stochastic nature of domain nucleation with respect to an applied magnetic field, we have determined the correlation coefficient among different domain configurations obtained from the repeated experiments. The correlation coefficient, *r*, was obtained from an analysis of domain configurations, represented by black nucleation sites and background noise, using the following equation:

$$r = \frac{\sum X_{ij} Y_{ij}}{\sqrt{(\sum X_{ij}{}^2)(\sum Y_{ij}{}^2)}}.$$

Here, X and Y are the matrices with the same size, where the matrix elements are represented by 1 or 0 on the basis of existence or nonexistence of domain nucleation in each pixel with a size of 10 nm x 10 nm. We consider that domain is nucleated when the signal is larger than the average of background noise. Thus, background noise without domain nucleation is not contributed to the correlation coefficient. The correlation coefficient is 0, when the domain nucleation configurations are totally different. Whereas, it becomes 1, when the domain nucleation configurations are completely identical. In Figs. 3(a) and (b), we plot the correlation coefficient with respect to an applied magnetic field in the ascending and descending branches of the major hysteresis loop, respectively. We note that the correlation coefficient in the both cases increases as the strength of an applied magnetic field increases, in the ascending and descending branches of the major hysteresis loop. This is naturally expected, since more nucleated domains are existed with approaching to the remnant state. A similar trend is also found in the correlation coefficient of domain configuration with inversion of the applied field in the right and left branches of the major hysteresis loop, as shown in Fig. 3(c). We have confirmed that the value of the correlation coefficient and its dependence on an applied field were similar in the other samples with different compositions. Therefore, nearly stochastic process in magnetization reversal is believed to be a universal behavior in nanogranular thin films.

It is quite surprising that the CoCrPt alloy film, which has numerous pinning sites at the grain boundaries mainly due to compositional segregation, shows a nearly stochastic behavior in domain nucleation. One might have expected a deterministic behavior of domain nucleation in the heavily disorder system for example due to surface roughness and/or compositional inhomogeneity [16,17]. Our experimental results strongly suggest that the thermal effects rather than the pinning effect dominate the domain nucleation process in CoCrPt alloy films. To confirm our conjecture we have carried out nanomagnetic simulations for the magnetization reversal process of CoCrPt alloy film using the OOMMF software [18]. We have used the stochastic Landau-Lifshitz-Gilbert equation for nanomagnetic simulation in the following form [19]:

$$\frac{d\vec{M}}{dt} = -|\gamma|\vec{M}\times\left(\vec{H_{eff}}+\vec{h_{fluct}}\right)-\frac{|\gamma|\alpha}{M}\vec{M}\times\left(\vec{M}\times\left[\vec{H_{eff}}+\vec{h_{fluct}}\right]\right),$$

where γ is a gyromagnetic ratio and α is dimensionless damping coefficient parameter that measures the magnitude of the relaxation term relative to the gyromagnetic term in the dynamical equation. In this equation the thermal effect is reflected by considering a fluctuating magnetic field h_{fluc}, which is caused by fluctuations of the magnetic moment orientation due to interaction of the magnetic moment with conducting electrons, phonons, nuclear spins, etc. [20]. The variance of fluctuation in the magnetic field is given by $V_{ar} = \frac{\alpha}{1+\alpha^2}\cdot\frac{2k_BT}{\gamma\mu_0 M_s V}$, which is derived from Brown's Fokker-Planck equation [21]. In the simulation, thermal fluctuations of the magnetic field are generated by a random number on each site. A different number corresponds to a different fluctuation value within the variance of fluctuation in the magnetic field. The random numbers for each site are generated in time step of every 4×10^{-15} sec and the number is statistically independent from the previous one. In the simulation, we have considered the detailed nanostructure of the sample. For this, the original SEM image of CoCrPt alloy film was converted into two level images composed of white grains and black grain boundaries. We have performed an image processing with the converted image to generate the sample image for nanomagnetic simulation. The processed image consists

of grains indexed by different gray levels and grain boundaries. Nanomagnetic simulation using OOMMF has been carried out with a cell size of 10×10 nm^2 in a 400×400 nm^2 sample area. As material parameters for the simulation, the measured values of uniaxial magnetic anisotropy $K_u = 6.8 \times 10^6$ *erg/cc*, saturated magnetization M_s = 480 *emu/cc*, and the exchange constant $A_{ex} = 1.5 \times 10^{-5}$ *erg/cm* of pure Co were used for the grains, while smaller values of $K_u = 2 \times 10^6$ *erg/cc*, M_s=160 *emu/cc*, and $A_{ex} = 2.5 \times 10^{-6}$ *erg/cm* were used for the grain boundaries. The smaller values of K_u, M_s, and A_{ex} at grain boundaries were chosen than those in the grains considering the fact that the magnetic anisotropy, saturated magnetization, and exchange interaction, are proportionally decreased with the amount of Cr segregated at grain boundaries [22].

We have simulated the magnetization reversal patterns with repeated hysteretic cycles at T=300 K. Four consecutive domain reversal patterns taken at applied magnetic fields of +700, +500, +350, +200, +100, and 0 Oe in the descending branch of the simulated hysteresis loop are observed in Fig. 4. One clearly notices that the magnetization reversal patterns obtained from the repeated simulations are mostly uncorrelated as seen in the experimental observations. To quantitatively compare our simulation results with the experimental ones we estimate the correlation coefficient among magnetization reversal patterns. The correlation coefficient in the simulations is changed from 0 to 0.40 ± 0.03 with varying an applied magnetic field from +700 to 0 Oe, which is well matched to the experimental values from 0.08 ± 0.02 to 0.38 ± 0.03 with changing a magnetic field from +620 to +5 Oe in the descending branch of hysteresis loop within the experimental error. Separately, we have confirmed that magnetization reversal patterns at T=0 K are completely deterministic for repeated nanomagnetic simulations, however there are no experiments at T=0 K so far.

We report here the first direct experimental observation of the nealy stochastic nature of magnetization reversal process on a nanometer length scale in high-density magnetic recording media of CoCrPt alloy film. Thermal fluctuations in the orientation of the

magnetic moments of the grains are found to play a dominant role in the stochastic behavior of domain nucleation during magnetization reversal of CoCrPt alloy film.

Acknowledgements

This work was supported by the Ministry of Science and Technology of Korea through the Basic Research Project, the Cavendish-KAIST Research Cooperation Project and by the Director, Office of Science, Office of Basic Energy Sciences, Materials Sciences and Engineering Division, of the U.S. Department of Energy under Contract No. DE-AC02-05CH11231.

References

[1]. M. Mansuripur, The Physical Principles of Magneto-optical Recording (Cambridge University Press, New York, 1995), pp. 543-676.

[2]. A. Hulbert and R. Schaefer, Magnetic Domains (Springer, Berlin, 1998).

[3]. J. M. Deutsch, A. Dhar, and O. Narayan, Phys. Rev. Lett. **92**, 227203-1 (2004).

[4]. K. Ohashi, H. Takagi, S. Tsunashima, T. Fujii and S. Uchiyama, J. Appl. Phys. **50**, 1611 (1979).

[5]. J. R. Petta, M. -B. Weissman, and G. Durin, Phys. Rev. E **56**, 2776 (1997).

[6]. P. Cizeau, S. Zapperi, G. Durin, and H. E. Stanley, Phys. Rev. Lett. **79**, 4669 (1997).

[7]. M. S. Pierce, R. G. Moore, L. B. Sorensen, S. D. Kevan, O. Hellwig, E. E. Fullerton, and J. B. Kortright, Phys. Rev. Lett. **90**, 175502 (2003).

[8]. M. S. Pierce, R. G. Moore, L. B. Sorensen, S. D. Kevan, O. Hellwig, E. E. Fullerton, and J. B. Kortright, Phys. Rev. Lett. **94**, 017202-1 (2005).

[9]. P. Fischer, G. Schütz, G. Schmahl, P. Guttmann, and D. Raasch, Z. f. Physik B **101**, 313 (1996).

[10]. W. Chao, B. H. Harteneck, J. A. Liddle, E. H. Anderson, and D. T. Attwood, Nature **435**, 1210-1213 (2005).

[11]. D. -H. Kim, Peter Fischer, Weilun Chao, Mi-Young Im, Sug-Bong Choe, Sung-Chul Shin, and Erik Anderson, J. Appl. Phys. **99**, 08H303 (2006).

[12]. Y. Matsuda, Y. Yahisa, J. Inagaki, and A. Ishikawa, J. Appl. Phys. **79**, 5351 (1996).

[13]. P. Fischer *et al.*, Rev. Sci. Instr. **72(5)**, 2332 (2001).

[14]. M. - Y. Im, D. -H. Kim, and S. -C. Shin, Phys. Rev. B **72**, 132416 (2005).

[15]. M. -Y. Im, P. Fischer, T. Eimüller, G. Denbeaux, S. -C. Shin, Appl. Phys. Lett. **83**(22), 4589 (2003).

[16]. N. Inaba and M . Futamoto, J. Appl. Phys. **87**, 6863 (2000).

[17]. E. Vives and A. Planes, Phys. Rev. B **63**, 134431 (2001).

[18]. M. J. Donahue and D. G. Porter, OOMMF Users Guide Version 1.2a3.

[19]. J. L. Garcia-Palacios and F. J. Lazaro, Phys. Rev. B **58**, 14937 (1998).

[20]. L. Neel, Ann. Geophys. **5**, 99 (1949).

[21]. W. F. Brown, Phys. Rev. **130**, 1677 (1963).

[22]. K. Kimoto, Y. Yahisa, T. Hirano, K. Usami, and S. Narishige, Jpn. J. Appl. Phys. **34**, 352 (1995).

Figure Captions

FIG. 1. (a) Typical magnetic domain configuration of $(Co_{83}Cr_{17})_{87}Pt_{13}$ alloy film recorded at the Co L_3 absorption edge (777 eV) with an applied magnetic field of +400 Oe. (b) M vs H hysteresis loop obtained via VSM measurement.

FIG. 2. Magnetic domain configurations of $(Co_{83}Cr_{17})_{87}Pt_{13}$ alloy film taken (a) at applied magnetic fields of +620,+512, +383, +254, +124, and +5 Oe in the descending branch of the major hysteresis loop and (c) at applied magnetic fields of ±620, ±512, ±383, ±254, ±124, and ±5 Oe in the process of the hysteretic cycle, respectively. Overlapped domain configuration image in a larger sample area of $7.6 \times 7.6\ \mu m^2$ taken (b) at an applied magnetic field of +400 Oe and (d) at an applied magnetic field of ±400 Oe, respectively.

FIG. 3. The correlation coefficient with respect to an applied magnetic field in the (a) ascending and (b) descending branches of the major hysteresis. (c) The correlation coefficient among the domain configurations with inversion of an applied field in the right and left branches of the major hysteresis loop.

FIG. 4. The reversal patterns are taken at applied magnetic fields of +700, +500, +350, +200, +100, and 0 Oe in the descending branch of the simulated hysteresis loop for four consecutive hysteretic cycles at T=300 K.

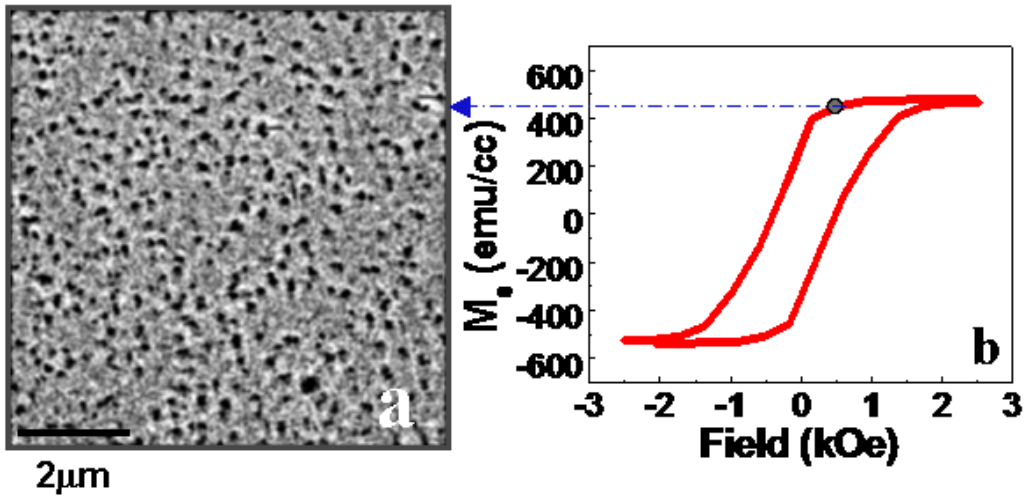

FIG. 1

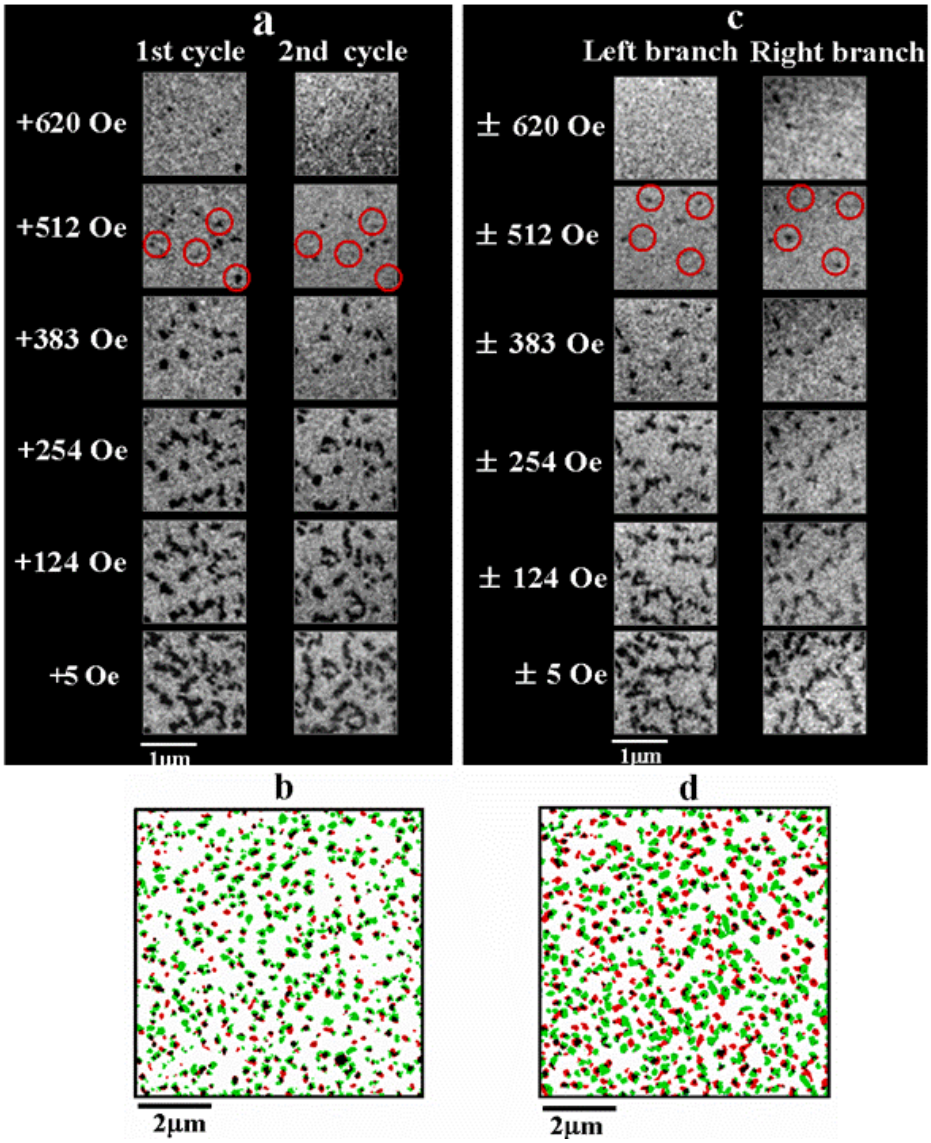
a
1st cycle
2nd cycle
+620 Oe
+512 Oe
+383 Oe
+254 Oe
+124 Oe
+5 Oe
1μm
c
Left branch
Right branch
± 620 Oe
± 512 Oe
± 383 Oe
± 254 Oe
± 124 Oe
± 5 Oe
1μm
b
2μm
d
2μm

FIG. 2

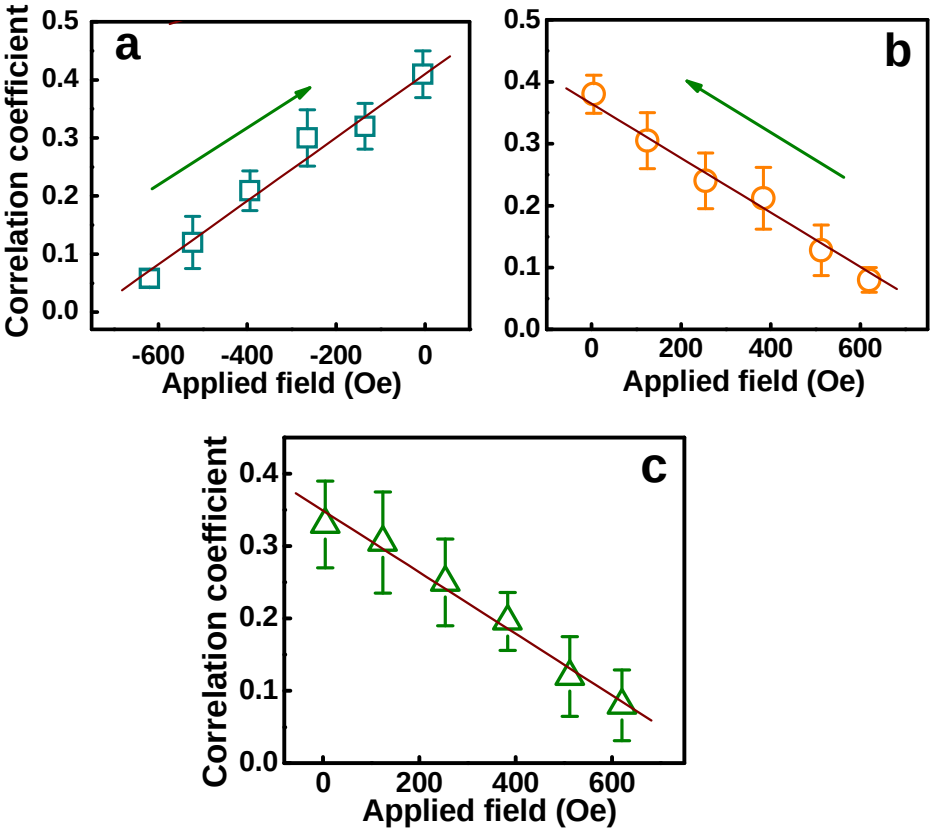
a
b
c
Correlation coefficient
Applied field (Oe)
0.0
0.1
0.2
0.3
0.4
0.5
-600
-400
-200
0
200
400
600

FIG. 3

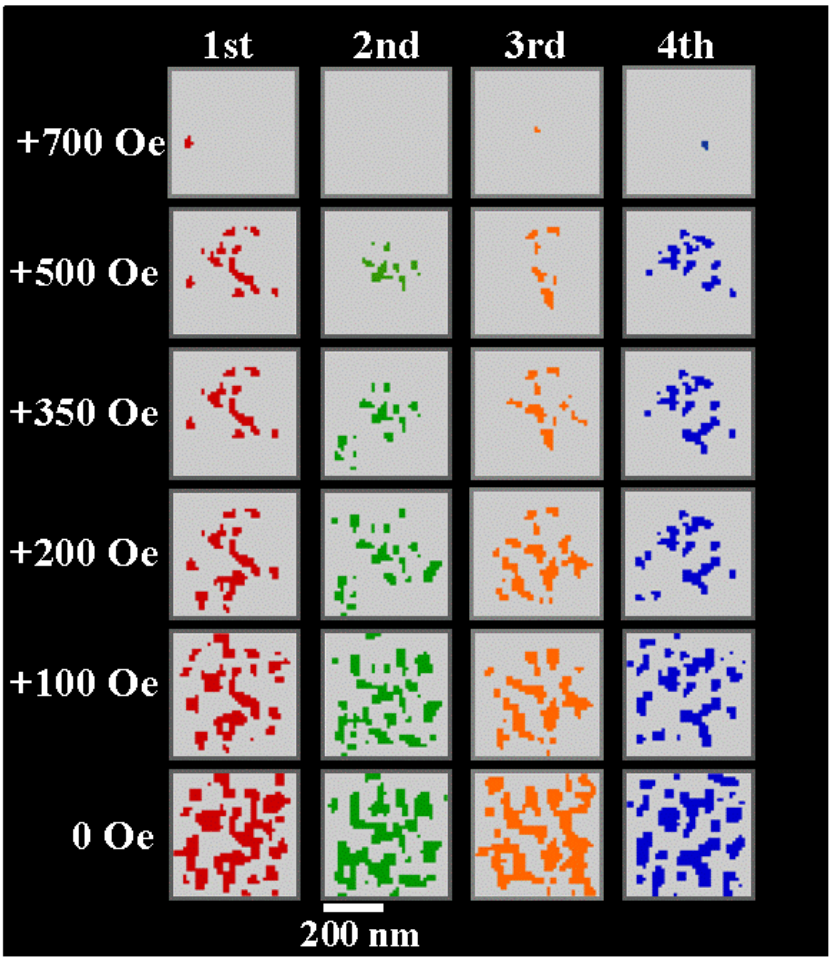

FIG. 4